

## Chapter 2

# Complex Modulus Variation by Manipulation of Mechanical Test Method and Print Direction

Megan L. Liu, Katherine K. Reichl, and Daniel J. Inman

**Abstract** 3D printing technologies have made creating prototypes with complex geometries relatively simple thus it has become an increasingly popular method for creating prototypes in a research setting. Therefore, it is crucial to understand the properties of the materials being used. This paper examines the effects of printing direction and testing method type on the complex modulus of viscoelastic materials printed using the Objet Connex 3D Printer from Stratasys. Because of its ability to print multiple materials in a single print job, this printer is a popular choice to create models. Throughout these tests the sample material will be kept constant to isolate the effects of print direction and test performed. DM 8430 is produced by mixing VeroWhitePlus™ and TangoPlus™ in a specific ratio. Since the 3D printer threads and smooths the sample uniaxially, the print direction of the sample can be manipulated by changing the orientation at which the sample is placed on the printer. Two different print directions, that are perpendicular with respect to each other, will be examined. The two test methods that will be used to determine the complex modulus are the Dynamic Mechanical Analysis (DMA) test, which examines the tensile behavior of the material, and the vibrating beam test, which examines the bending behavior. The goal is to gain greater insight into the uncertainty in the complex modulus that results from changing the test and printing direction used to determine this value. This will be done by performing a total of four tests. For each testing method, DMA and vibrating beam, the complex modulus will be found for two samples of different print direction, vertical and horizontal. These results will permit a greater understanding of the amount of variability produced by print direction.

**Keywords** Additive manufacturing • Complex modulus • Viscoelastic • Passive damping • Dynamic modulus analysis

## 2.1 Introduction

Additive manufacturing has become increasing popular across almost all engineering fields. The field of interest to the authors is in applications for metastructures to be used for vibration suppression [1, 2]. The specific printer of interest is the Objet Connex printer which is capable of printing rubber-like materials. These materials exhibit viscoelastic properties which is of particular interest for vibration suppression [3]. The purpose of this paper is towards the determination of the viscoelastic properties of the printed materials.

The Object Connex printer uses PolyJet printing technology which works like an inkjet printer. The parts are made by depositing many small dots of material and then curing the resin resulting in an end material that appears homogenous. Because of the digital nature of this method, these materials are referred to as digital materials (DM). This method allows the printer to easily mix two different base materials in various ratios to create a gradient of material with various hardness levels [4]. This method also allows for parts made in a single print with both rigid and viscoelastic materials.

Using this technique and the many base materials available, the Object Connex printer has the capability to create many materials but for this paper the focus will be on the digital materials created using the two base materials, VeroWhitePlus™ and TangoPlus™. VeroWhitePlus™ is a rigid opaque material and TangoPlus™ is a rubber-like transparent material [5]. Using these two base materials, ten different digital materials can be created [6]. The material studied here is DM 8430 which is the third stiffest material. In the field of active composites and origami, H. Jerry Qi has done extensive work using the Objet Connex 3D printer and his papers provide many details the actual mechanisms the 3D printer utilizes [7].

---

M.L. Liu

Department of Material Science and Engineering, University of Michigan, François-Xavier Bagnoud Building,  
1320 Beal Avenue, Ann Arbor, MI 48109, USA

K.K. Reichl (✉) • D.J. Inman

Department of Aerospace Engineering, University of Michigan, François-Xavier Bagnoud Building,  
1320 Beal Avenue, Ann Arbor, MI 48109, USA  
e-mail: reichl@umich.edu

**Fig. 2.1** Schematic of print directions utilized (a) horizontal direction (b) vertical direction

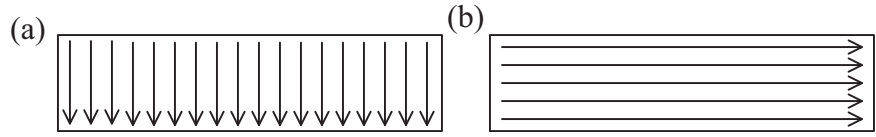
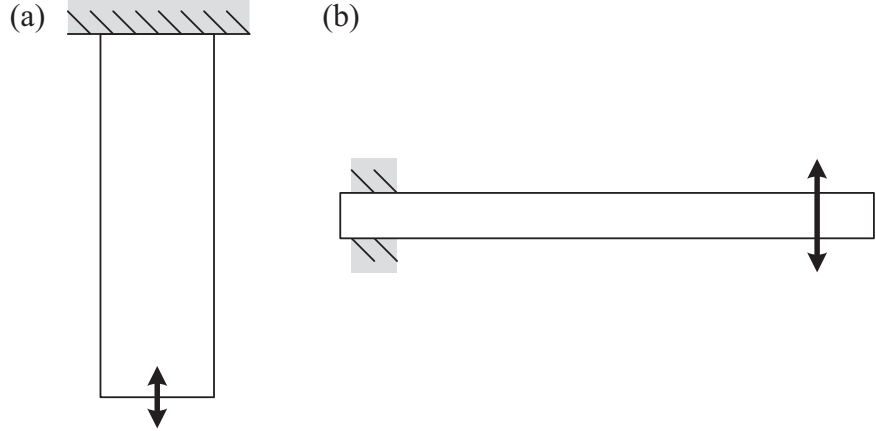


**Fig. 2.2** Schematic of testing configurations utilized (a) tensile configuration (b) single cantilever configuration



In this paper, two different print directions are studied in addition to two different testing configurations. The two print directions are depicted in Fig. 2.1 where the arrows represent the direction in which the material was printed. The Object Connex always prints parallel rows of materials. The reasoning behind these two testing methods is to determine how these the print direction affects the dynamic modulus properties. The print direction creates visible differences in the parts.

Two different testing configurations were utilized to determine the effects of the testing configuration. One sample was tested in tension and the other was tested using the single cantilever orientation (Fig. 2.2). The storage modulus, loss modulus, and loss factor values obtained from these tests are compared and the differences that result from a change in testing method and print direction are analyzed.

## 2.2 Viscoelastic Material Behavior

The viscoelastic phenomenon can be seen in the dynamic response of a viscoelastic material due to a sinusoidal load. For an elastic material if a harmonically varying stress is applied to the material, the strain response will be at that same frequency and it phase with the load. For a viscoelastic material this is not the case. The response is still at the same frequency as the input but has a phase lag. If a time-varying stress  $\sigma(t)$  is applied to a viscoelastic material as follows

$$\begin{aligned}\sigma(t) &= \sigma_0 \sin(\omega t) \\ \varepsilon(t) &= \varepsilon_0 \sin(\omega t - \delta)\end{aligned}\tag{2.1}$$

where  $\omega$  is the frequency of the forcing function and strain-response of the material is  $\varepsilon(t)$ . The phase lag is denoted as  $\delta$ . From these relationships, a dynamic stiffness (or complex stiffness) can be expressed as a complex number.

$$\frac{\sigma(t)}{\varepsilon(t)} = E'(\omega) + i E''(\omega) = E(\omega)[1 + i \mu(\omega)]\tag{2.2}$$

where  $E'$  is called the storage modulus and  $E''$  is known as the loss modulus. The modulus can also be expressed by factoring out the storage modulus which leaves the loss factor,  $\mu$ . The modulus values vary with both frequency and temperature [8].

Using the time-frequency equivalence, we can assume that the complex modulus value at a frequency,  $f_1$  and a temperature  $T_1$  is equal to the value at any other frequency  $f_2$  and some temperature  $T_2$  such that the following relationship can be made

$$E(f_1, T_1) = E(f_2 \alpha(T_2)) \quad (2.3)$$

where  $\alpha(T_2)$  is called the shift factor and describes the relationship between frequency and temperature. Using the shift factor, the effects of both temperature and frequency can be combined into a single variable known as the reduced frequency,  $f_r(f, T) = f\alpha(T)$ . The shift factor relationship is determined by testing a material at multiple frequencies and temperatures. For each temperature, a shift factor value is determined graphically by examining the modulus versus reduced frequency plots. Varying the shift factor causes the data at that temperature to shift on the reduced frequency scale. Once the shift factors for each temperature are determined, the  $\log[\alpha(T)]$  is plotted versus  $1/T$ . This relationship resembles a slightly curved line, which here is approximated as straight line and the Arrhenius shift factor equation is fit to the data. The Arrhenius shift factor equation takes on the following form

$$\log[\alpha(T)] = T_A \left( \frac{1}{T} - \frac{1}{T_0} \right) \quad (2.4)$$

where  $T_0$  is any arbitrarily selected reference temperature and  $T_A$  is the slope of the line and is related to the activation energy. Using this relationship, the complex modulus and loss factor can be expressed as follows

$$E(f, T) = E \left[ f \exp \left( -2.303 T_A / T \right) \exp \left( 2.303 T_A / T_0 \right) \right] \quad \eta(f, T) = \eta \left[ f \exp \left( -2.303 T_A / T \right) \exp \left( 2.303 T_A / T_0 \right) \right] \quad (2.5)$$

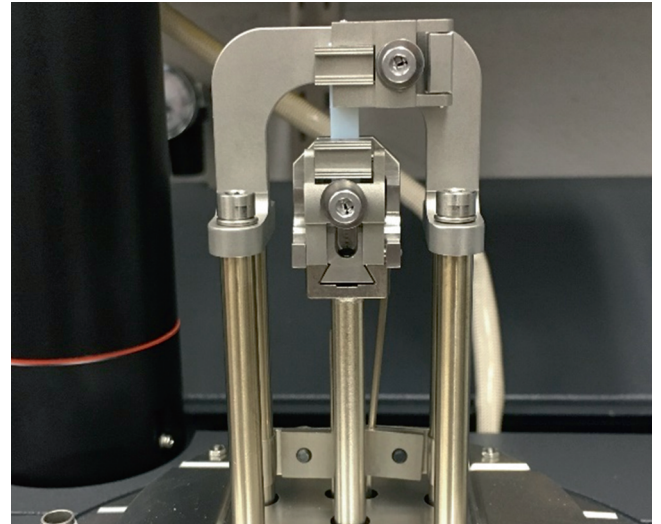
### 2.3 Testing Methods

The complex modulus of the DM 8430 material was obtained using the Dynamic Mechanical Analysis (DMA) Q800 machine by Thermal Analysis using the tensile and single cantilever configurations as explained above. Two samples were tested for each configuration each which used a different print direction.

For the tensile configuration, the testing procedure followed the ASTM D5026 standard [9]. Figure 2.3 shows a setup of the of test. The sample specimen was held in place by two clamps, the upper of which was fixed while the bottom moved cyclically. Both samples were tested at 9 temperatures varying linearly between 25 and 105 °C. A soak time of 5 min was used at each temperature to ensure the sample reached the isothermal state. At each temperature, the sample was tested at 13 frequencies varying logarithmically between 100 and 0.10 Hz. The dimensions of the samples were approximately  $9.5 \times 1 \times 5$  mm.

Using the cantilevered configuration, the sample was tested in flexure using the Q800 single cantilever fixture. This procedure closely follows the ASTM D5418 standard. The standard presented pertains to a dual cantilever beam and here a single cantilever was used [10]. A fixed clamp held one side of the beam, and the other moved cyclically at the specified frequency of the test sequence. These samples were tested at 9 temperatures varying linearly between 35 and 90 °C once

**Fig. 2.3** DMA tension test configuration



again with a soak time of 5 min. At each temperature, the specimen was tested at 10 frequencies varying logarithmically between 18 and 0.10 Hz. The cantilevered specimens had dimension of  $35 \times 3 \times 12$  mm.

The DMA Q800 software collects and analyzes the data for each temperature and frequency. Based on the geometry of the testing specimen, the software outputs the storage modulus and the loss factor for the material at the specified temperatures and frequencies. Next, the data is manually analyzed further to determine the relationship between temperature and frequency. The shifting procedure described above is used to determine the relationship between the shift factors,  $\alpha$  and the temperature  $T$ . This allows the complex modulus data to be plotted against a single variable, reduced frequency. For all tests a reference temperature of  $65^\circ\text{C}$  was used. The parameters for the best fit line for the Arrhenius fit is also reported.

## 2.4 Results

The final shifted results from all four of the configurations tested are presented in this section these configurations are summarized in Table 2.1. The results for the tensile configuration are shown in Figs. 2.4 and 2.5 and for the cantilevered configuration are shown in Figs. 2.6 and 2.7. The complex modulus values are plotted versus reduced frequency and the logarithmic value of shift factor used to determine the reduced frequency are plotted versus the inverse of the temperature along with the Arrhenius fit. The values of the Arrhenius fit line are reported in Table 2.1.

From these plots, the horizontal and the vertical printing directions are virtually indistinguishable from each other. The results lead us to believe that the in-place print direction does not affect the complex modulus values. Next, a comparison of the testing configurations is shown in Fig. 2.8. The testing configuration clearly makes a difference in the complex modulus values of the material. This difference is much more noticeable in the storage modulus values than the loss factor data. In the loss factor data, the peak in the tensile configuration data has a higher value than that of the cantilever configuration.

**Table 2.1** Arrhenius shift factor equation fit

Configuration	Printing direction	Reference temperature [ $^\circ\text{C}$ ]	Arrhenius temperature [K]
Tensile	Horizontal	65	12,372
Tensile	Vertical	65	12,804
Cantilever	Horizontal	65	14,472
Cantilever	Vertical	65	15,667

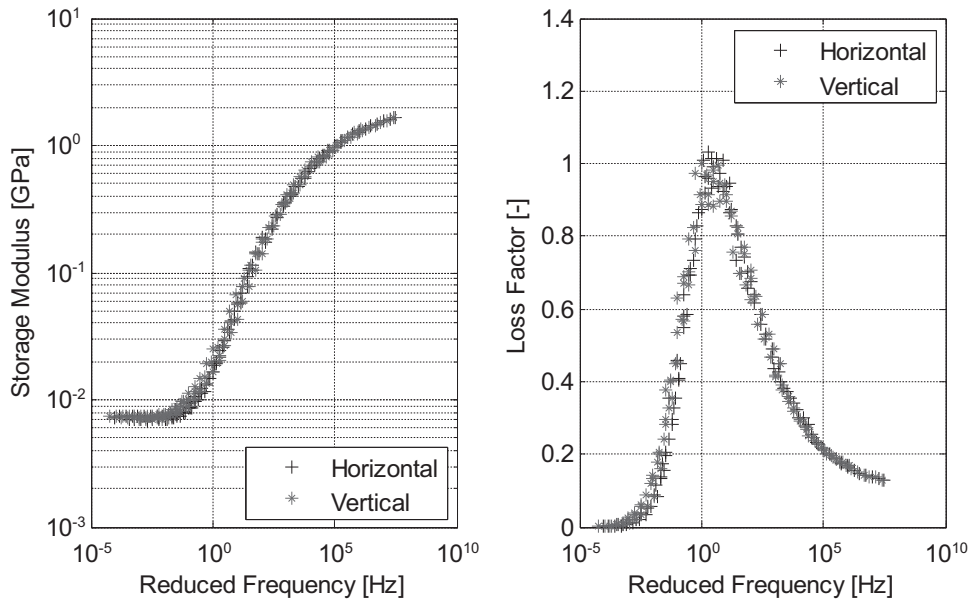


**Fig. 2.4** Complex modulus plots for the vertical and horizontal printing directions of the tensile configuration with a reference temperature of  $65^\circ\text{C}$

**Fig. 2.5** Shift factor relationship and Arrhenius fit for the tensile configuration

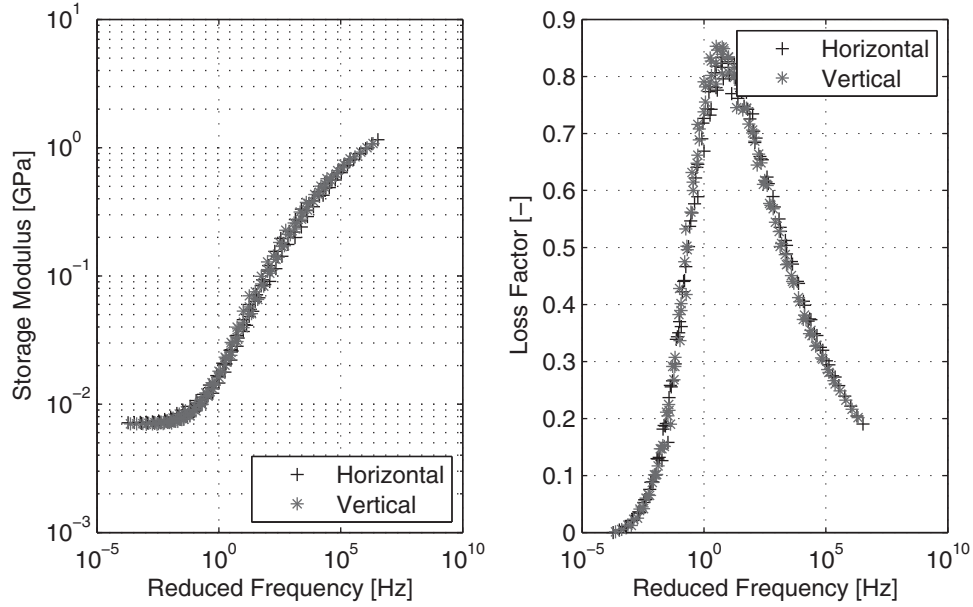
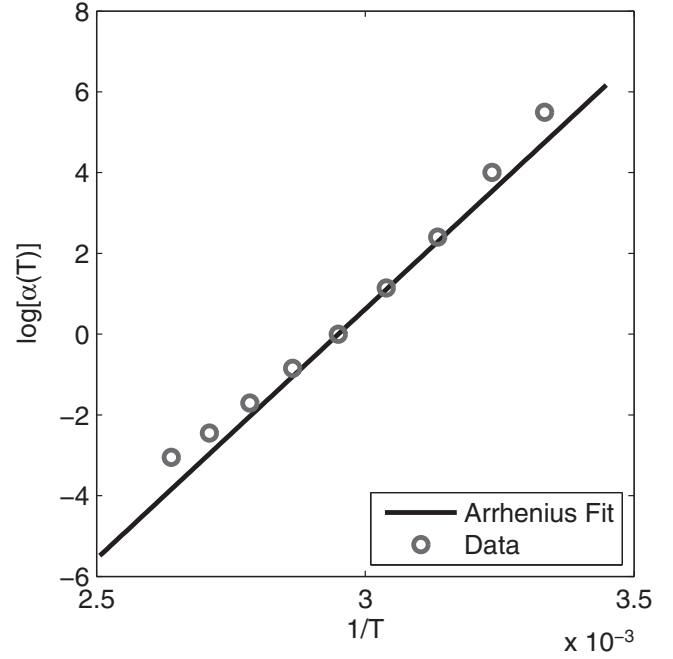


**Fig. 2.6** Complex modulus plots for the vertical and horizontal printing directions of the cantilevered configuration with a reference temperature of 65 °C

## 2.5 Conclusions

Firstly, this work shows that the DM 8430 material exhibits significant viscoelastic material behavior which should be taken into consideration when modelling this material. This is particularly important when temperature change is occurring. In addition, this work provides valuable insight into the effects of print direction on the modulus properties of the material. The results show that variations in the in-plane print direction does not affect the response of the material. This was demonstrated in both the tensile and cantilevered configurations. The testing configuration does affect the complex modulus values, thus when using this data for modeling the configuration that most closely resembles the structure being modeled should be used.

**Fig. 2.7** Shift factor relationship and Arrhenius fit for the cantilevered configuration

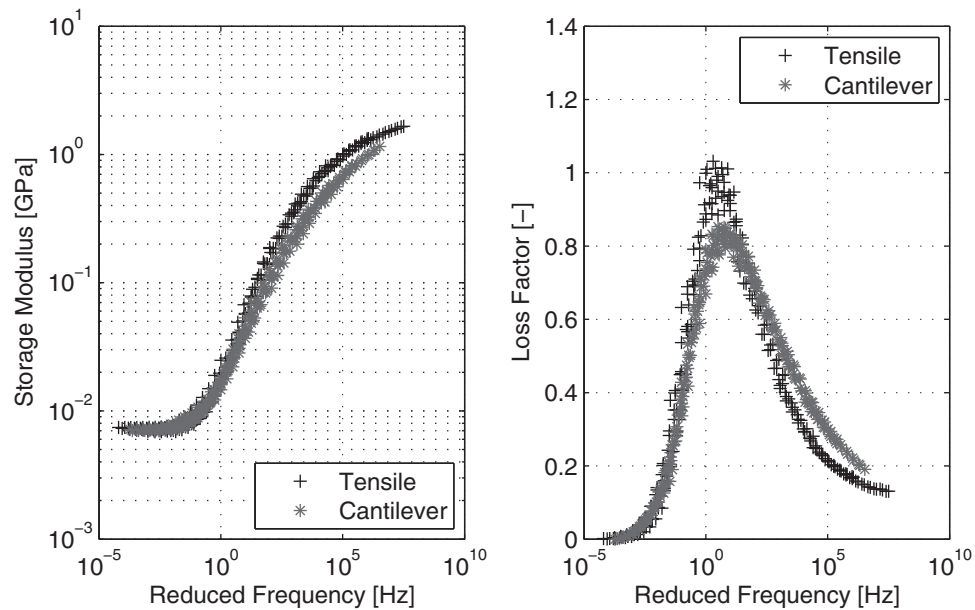
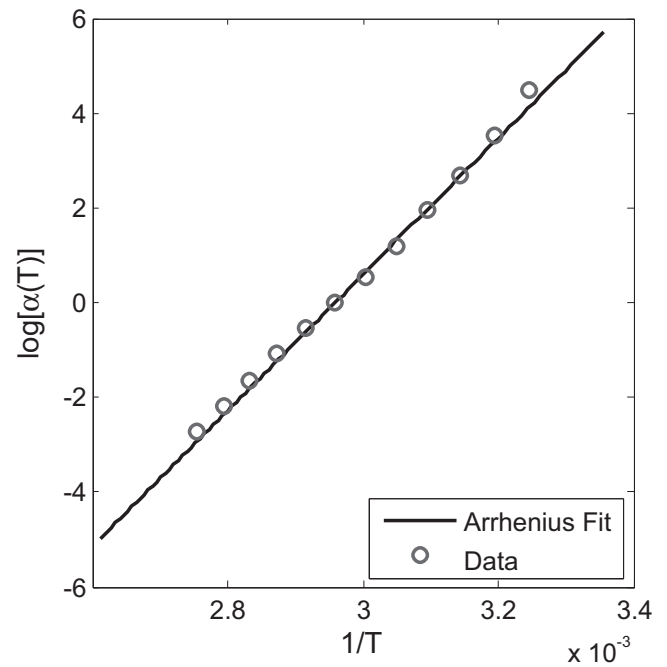


**Fig. 2.8** Complex modulus data comparing the tensile and cantilevered configurations with a reference temperature of 65 °C

**Acknowledgements** This work is supported in part by the US Air Force Office of Scientific Research under the grant number FA9550-14-1-0246 “Electronic Damping in Multifunctional Material Systems” monitored by Dr. BL Lee and in part by the University of Michigan.

## References

1. Reichl, K. K., Inman, D. J.: Modelling of low-frequency broadband vibration mitigation for a bar experiencing longitudinal vibrations using distributed vibration absorbers. In: 20th International Conference on Composite Materials, Copenhagen, 2015
2. Hobeck, J. D., Laurant, C. M. V., Inman, D. J.: 3D printing of metastructures for passive broadband vibration suppression. In: 20th International Conference on Composite Materials, Copenhagen, 2015
3. Ge, Q., Dunn, C.K., Qi, H.J., Dunn, M.L.: Active origami by 4D printing. *Smart Mater. Struct.* **23**(94007), 1–15 (2014)

4. Objet Connex 3D Printers [Online]. Available: <http://www.stratasys.com/3d-printers/design-series/connex-systems> (2015). Accessed 17 Oct 2015
5. Stratasys PolyJet Materials Data Sheet [Online]. Available: [http://usglobalimages.stratasys.com/Main/Secure/Material Specs MS/PolyJet-Material-Specs/Digital\\_Materials\\_Datasheet.pdf?v=635581278098921962](http://usglobalimages.stratasys.com/Main/Secure/Material%20Specs%20PolyJet-Material-Specs/Digital_Materials_Datasheet.pdf?v=635581278098921962) (2014). Accessed 17 Oct 2015
6. Stratasys Digital Materials Data Sheet [Online]. Available: [http://usglobalimages.stratasys.com/Main/Secure/Material Specs MS/PolyJet-Material-Specs/Digital\\_Materials\\_Datasheet.pdf?v=635581278098921962](http://usglobalimages.stratasys.com/Main/Secure/Material%20Specs%20PolyJet-Material-Specs/Digital_Materials_Datasheet.pdf?v=635581278098921962) (2015). Accessed 17 Oct 2015
7. Ge, Q., Mao, Y., Yu, K., Dunn, M. L., Qi, H. J.: Active composites and 4D printing. In: 20th International Conference on Composite Materials, Copenhagen, 2015
8. Lakes, R.S.: Dynamic behavior. In: Viscoelastic Materials, pp. 55–90. Cambridge University Press, New York (2009)
9. ASTM: Standard Test Method for Measuring the Plastics: Dynamic Mechanical Properties of Plastics in Tension Properties: In Tension 1, no. D5026 – 15, pp. 1–5. (2001)
10. ASTM: Standard Test Method for Plastics: Dynamic Mechanical Properties: In Flexure (Three-Point Bending), no. D5418 – 15, pp. 1–4. (2007)





Mechanics of Additive and Advanced Manufacturing,  
Volume 9

Proceedings of the 2017 Annual Conference on  
Experimental and Applied Mechanics

Wang, J.; Antoun, B.; Brown, E.; Chen, W.; Chasiotis, I.;  
Huskins-Retzlaff, E.; Kramer, S.L.B.; Thakre, P.R. (Eds.)  
2018, VIII, 107 p. 80 illus., 50 illus. in color., Hardcover  
ISBN: 978-3-319-62833-2